Journal of Quantitative Spectroscopy & Radiative Transfer 111 (2010) 810–816

Contents lists available at ScienceDirect

Journal of Quantitative Spectroscopy & Radiative Transfer

journal homepage: www.elsevier.com/locate/jqsrt

Note

On the use of principal component analysis to speed up radiative transfer calculations

Vijay Natraj *, Run-Lie Shia, Yuk L. Yung

MC 150-21, Division of Geological and Planetary Sciences, California Institute of Technology, Pasadena, CA 91125, USA

ARTICLE INFO

Article history:
Received 21 July 2009
Accepted 3 November 2009

Keywords:
Fast radiative transfer
Principal component analysis
Two-stream
Remote sensing

ABSTRACT

Radiative transfer is computationally expensive. However, it is essential to many applications, in particular remote sensing retrievals. Principal component analysis of the optical depth and single scattering albedo profiles has been proposed as a possible method to help ease the computational burden. Here we show how the technique could be applied to a practical problem of CO_2 retrievals from high spectral resolution measurements of reflected sunlight in three near infrared bands. We obtain a speed improvement of more than 50 fold (compared to monochromatic computations), while reproducing the radiances to better than 0.1% accuracy.

1. Introduction

Radiative transfer (RT) computations are necessary to solve various problems such as the transmission of ultraviolet (UV) radiation through the atmosphere and ocean, remote sensing, solar heating and infrared (IR) cooling processes, UV biological dose rates, greenhouse warming, haze layers in planetary atmospheres and ocean optics. However, full treatment of RT processes is computationally involved. Consequently, a lot of work has gone into speeding up RT calculations.

Several spectral sampling techniques have been proposed (see, e.g., [1] for an overview). However, the efficiency of these spectral mapping techniques is very low in typical inhomogeneous atmospheres. This motivates the need for a fast and accurate scheme to alleviate the computational burden. This is even more important if polarization is considered. Polarized RT calculations are important for the interpretation of satellite-based measurements such as those from GOME [2–7], SCIAMACHY [8] and GOSAT [9]. Neglecting polarization in a Rayleigh scattering atmosphere can produce errors as large as 10% in the computed intensities [10,11]. On the other hand, a full vector RT computation is 20–50 times slower than one neglecting polarization.

Natraj et al. [1] introduced a possible approach employing principal component analysis (PCA) of the optical properties that takes advantage of the inherent redundancy in line-by-line (LBL) computation. PCA is a decomposition of a signal or data set in terms of orthogonal basis functions which are determined from the data (see, e.g., [1,12–14]). This technique reduces multidimensional data sets to lower dimensions by eliminating redundancy in the data.

In this paper, we improve upon the methods used by Natraj et al. [1] to maximize the advantages of PCA. First, we automate the process. Second, we use a dedicated two-stream RT model. Third, we include polarization in the computations. Fourth, we compute single scattering efficiently using interpolation of the phase matrix rather than the expansion coefficients. In Section 2 we explain how PCA is used to separate the monochromatic intervals into bins and how the radiance is subsequently evaluated. The test scenarios used to evaluate the technique are described in Section 3. In Section 4, we evaluate the performance of PCA in speeding up RT computations.

* Corresponding author. Tel.: +1 626 395 6962; fax: +1 626 585 1917.
E-mail address: vijay@gps.caltech.edu (V. Natraj).

0022-4073/$ - see front matter © 2009 Elsevier Ltd. All rights reserved.
doi:10.1016/j.jqsrt.2009.11.004

Table 1
Aerosol, ice and water cloud optical depth (at 757.2155 nm) for the different scenarios.

Scenario	Aerosol optical depth (at 757.2155 nm)	Ice cloud optical depth (at 757.2155 nm)	Water cloud optical depth (at 757.2155 nm)
28	0.0652	0	0
174	0.0655	0.2183	0
256	0.0652	0.0009	0.2193
2558	0.1472	0	0

The scenario numbers are as in O'Brien et al. [23].

Table 2
Aerosol, ice and water cloud types for the different scenarios.

Scenario	Aerosol types	Ice cloud types	Water cloud types
28	Continental, oceanic	None	None
174	Continental, oceanic	ic_070, ic_080, ic_085, ic_090	None
256	Continental, oceanic	ic_040, ic_045, ic_050, ic_090	wc_004, wc_005
2558	Continental	None	None

For ice (water) cloud types, the nomenclature is ic(wc)_xxx, where xxx is the effective radius in microns. The scenario numbers are as in O'Brien et al. [23].

Table 3
Single scattering albedos (at 757.2155 nm) and location of the aerosol, ice and water cloud types used in the simulations.

Aerosol/cloud type	Single scattering Albedo (at 757.2155 nm)	Location (mbar)
Continental	0.8730	215–1000
Oceanic	1.0000	810–1000
ic_040	0.9997	85–105
ic_045	0.9997	120
ic_050	0.9996	140
ic_070	0.9995	270–335
ic_080	0.9996	370
ic_085	0.9996	370–405
ic_090	0.9996	440–710, 840–1000
wc_004	1.0000	480–635, 900
wc_005	1.0000	810–870

2. Binning and mapping to monochromatic radiance

As in the work of Natraj et al. [1], we perform PCA over the optical depth and single scattering albedo profiles. We use the following criteria to group the spectral intervals into bins for which the calculations are made:

$$c_1 < \ln\tau < c_2, \tag{1a}$$

$$c_3 < \omega_1 < c_4, \tag{1b}$$

where τ is the cumulative gas absorption optical depth and ω_1 is the single scattering albedo of the top layer. c_1, c_2, c_3 and c_4 are parameters that depend on the spectral region and the required accuracy. The gas absorption optical depth is used rather than the total extinction optical depth because the former has much more significant spectral variation than scattering due to aerosols, clouds and air molecules. Further, the aerosol loading can vary substantially from scene to scene and it is desirable not to change the binning parameters for every scene. The single scattering albedo parameter accounts for the vertical structure of gas absorption.

Four EOFs were found to be adequate to capture more than 99.99% of the variance in the optical properties [1]. To reproduce the monochromatic radiance, we first introduce the following quantities:

$$I_d^0 = \ln(I^0/I_2^0), \tag{2}$$

$$I_{d,k}^+ = \ln(I_k^+/I_{2,k}^+), \tag{3}$$

$$I_{d,k}^- = \ln(I_k^-/I_{2,k}^-), \tag{4}$$

$$Q_d^0 = Q^0 - Q_1^0, \tag{5}$$

$$Q_{d,k}^+ = Q_k^+ - Q_{1,k}^+, \tag{6}$$

$$Q_{d,k}^- = Q_k^- - Q_{1,k}^-. \tag{7}$$

I and Q are Stokes parameters [15]. Subscripts k, 1 and 2 refer to the kth EOF, singly scattered radiance and two-stream computation, respectively; superscripts 0, + and − indicate radiance computations performed using the mean optical properties, and optical properties positively and negatively perturbed by one EOF, respectively.

The use of logarithm for the intensity calculation offers two advantages: negative intensities are automatically avoided, and the fact that extinction is exponential in the absence of scattering is taken into account.

Applying PCA to the ratio of n-stream and two-stream intensities—where stream refers to the number of quadrature angles for the RT computation—instead of the n-stream values alone reduces the number of terms needed in the PCA expansion for a fixed accuracy. This is because the radiation intensity is a complicated nonlinear function of the optical depth and single scattering albedo. PCA is a linear expansion method and is not very effective for nonlinear systems. The two-stream model computes the absorption perfectly in the absence of scattering. Considering scattering as a perturbation to gaseous absorption, the ratio of n-stream and two-stream intensities is almost linearly dependent on the optical parameters.

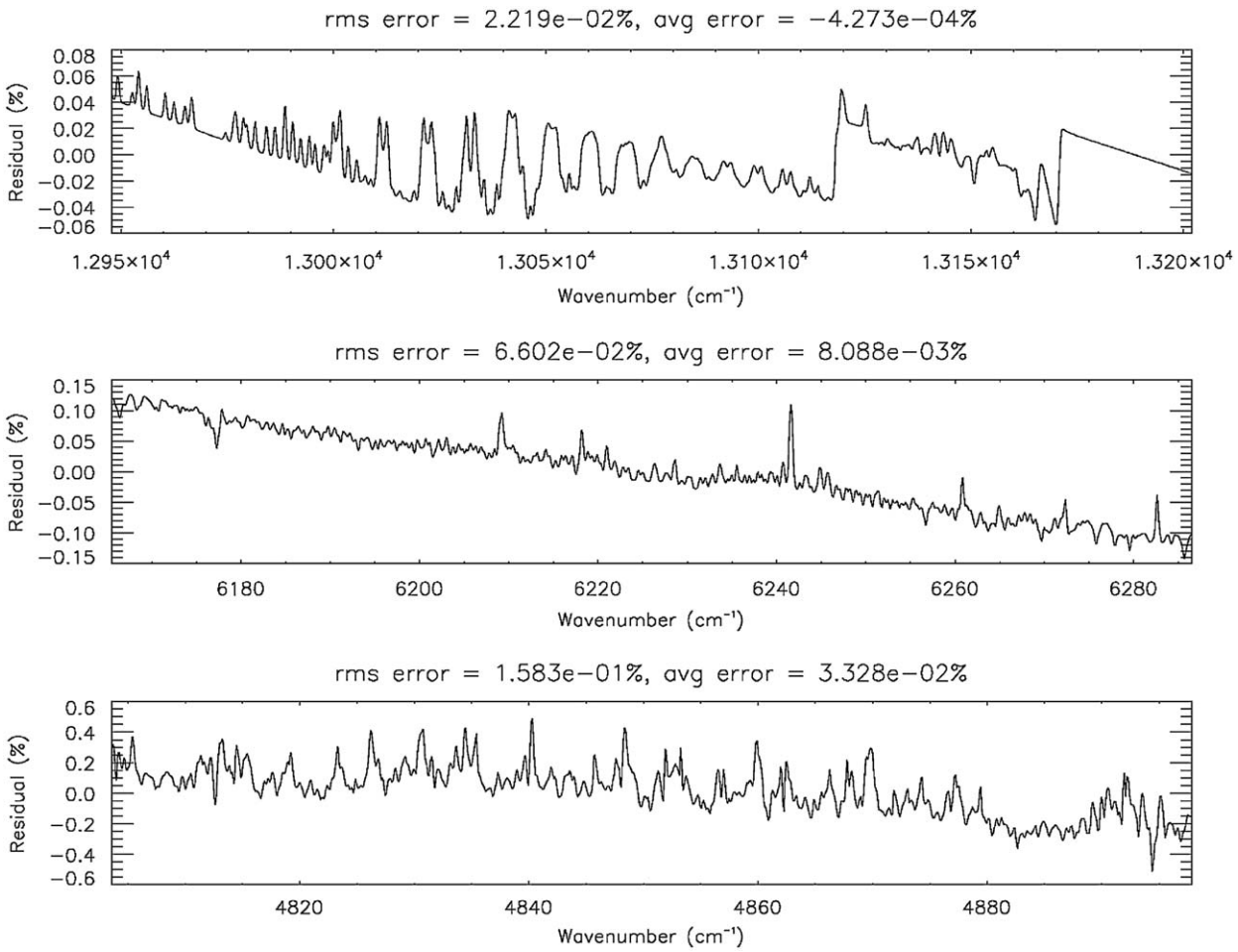

Fig. 1. Radiance error (for scenario 256) in Stokes parameter I in (top) O_2 A band; (middle) 1.61 μm CO_2 band; (bottom) 2.06 μm CO_2 band. The error is defined as (PCA–LBL)/LBL × 100.

Polarization, on the other hand, is a direct result of scattering (pure absorption is unpolarized). Typically, single scattering contributes significantly to the total polarization since multiple scattering is depolarizing. Hence, applying PCA to the multiply scattered polarized radiance gives excellent results.

The first and second order central differences can then be computed as follows:

$$\delta I_k = \frac{I^+_{d,k} - I^-_{d,k}}{2}, \tag{8}$$

$$\delta^2 I_k = I^+_{d,k} - 2I^0_d + I^-_{d,k}, \tag{9}$$

$$\delta Q_k = \frac{Q^+_{d,k} - Q^-_{d,k}}{2}, \tag{10}$$

$$\delta^2 Q_k = Q^+_{d,k} - 2Q^0_d + Q^-_{d,k}. \tag{11}$$

Finally, the radiances can be obtained:

$$I_l = I_2 \exp\left[I^0_d + \sum_k \delta I_k P_{kl} + \frac{1}{2}\sum_k \delta^2 I_k P^2_{kl}\right], \tag{12}$$

$$Q_l = Q_1 + Q^0_d + \sum_k \delta Q_k P_{kl} + \frac{1}{2}\sum_k \delta^2 Q_k P^2_{kl}, \tag{13}$$

where l is the wavenumber index.

3. Case study: reflected sunlight in the near infrared (NIR)

We employed PCA to simulate polarized backscatter measurements $\mathbf{I}=(I, Q, U, V)$ in NIR spectral regions relevant to space-based CO_2 retrieval [16], *viz.*, the 0.76 μm O_2 A band, and two vibration-rotation bands of CO_2 centered at 1.61 and 2.06 μm [17]. The intensity is computed using the multiple scattering scalar RT model LIDORT [18,19]. The dedicated two-stream model is based on a simplification of the discrete ordinates formalism for the special case of one upwelling and one downwelling quadrature direction (Spurr, private communication). The 2OS model [20,21] is used to account for polarization.

Four different scenarios were chosen from a database of ECMWF profiles [22], with different amount and vertical distribution of aerosols, ice and water clouds. Table 1 summarizes the cloud and aerosol optical

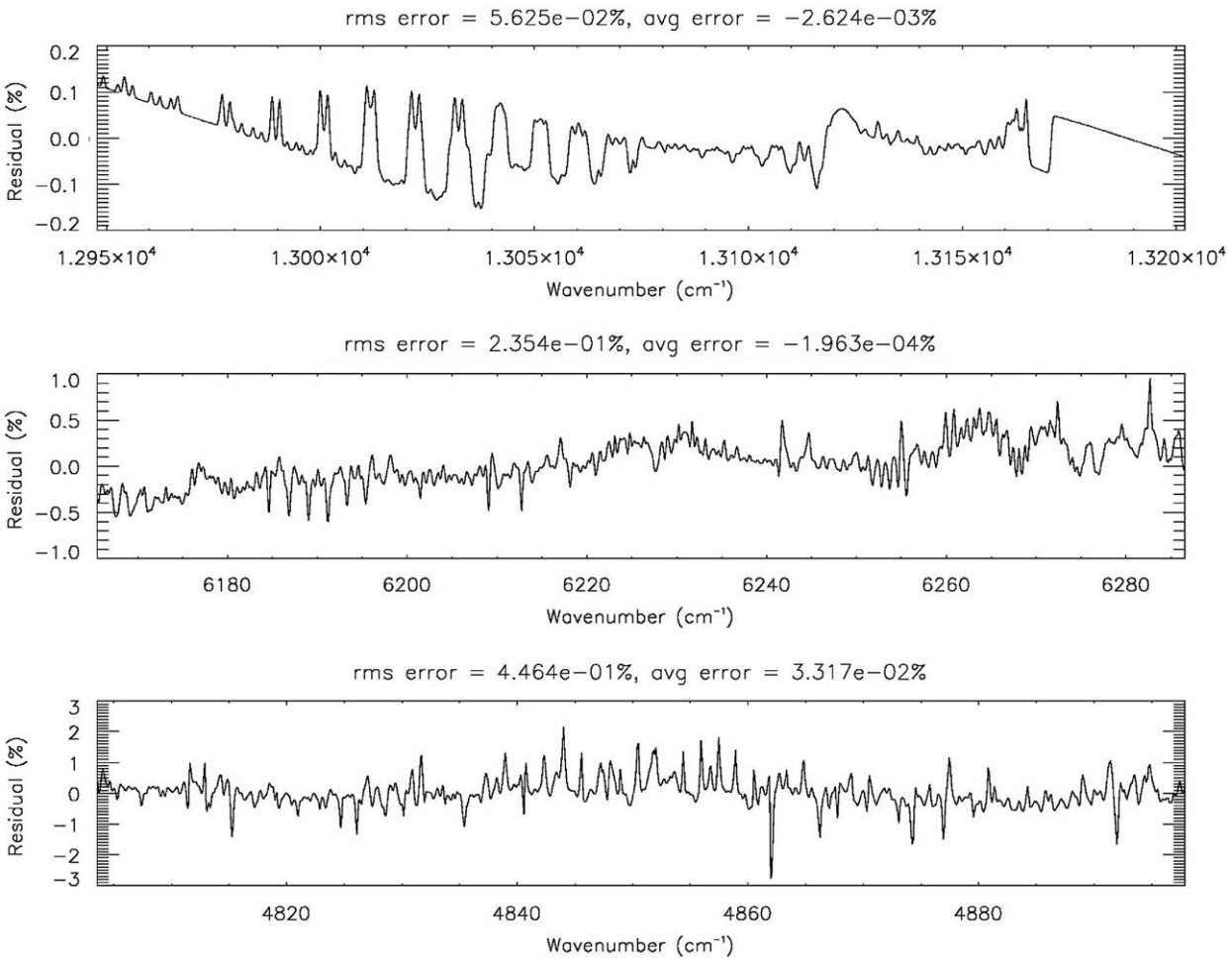

Fig. 2. Same as Fig. 1 but for Stokes parameter *Q*.

depths (at 757.2155 nm). Table 2 lists the aerosol and cloud types for each scenario. The single scattering albedos (at 757.2155 nm) and locations of the scatterers are presented in Table 3. The vertical distributions of cloud water and ice are drawn from O'Brien et al. [23], who used the ECMWF database prepared by Chevallier [22].

Single scattering is computed exactly and efficiently using interpolated values of the phase matrix at each wavelength as opposed to interpolating the expansion coefficients (which can have more than 1000 moments for large particles).

For the LBL computations, we use 16 streams—8 in each hemisphere. At least 16 streams are necessary to adequately capture the forward scattering by typical clouds and aerosols. The atmosphere is divided into 60 layers. The surface is considered to be Lambertian, with surface reflectance 0.1, 0.126 and 0.122 in the O_2 *A* band, the 1.61 μm CO_2 band and the 2.06 μm CO_2 band, respectively. The solar zenith angle, viewing zenith angle and relative azimuth angle are 50.3°, 50° and 0° respectively.

4. Results

We plot radiance errors for scenario 256 in Figs. 1–3. The errors are percentage differences between PCA and LBL computations. Figs. 1–3 show the errors for Stokes parameters *I*, *Q* and *I*–*Q*, respectively. The last quantity represents *s*-polarized radiation when the measurement is made in the principal plane, i.e., the plane containing the solar and viewing directions and the normal to the surface footprint. This is often more relevant to measurements than the individual Stokes parameters themselves. Note that this scenario is the worst case as it has 8 different aerosol/cloud types, all with different wavelength-dependence of scattering, and the total scattering optical depth is nearly 0.3. This is confirmed in Table 4, where the results for all scenarios are summarized.

Clearly, the errors (in *I*–*Q*) are only of the order of 0.1% (or less) even for this pathological case. There are three interesting features illustrated by these plots. First, there is a clear slope in the results. This is a direct consequence of the averaging of aerosol/cloud scattering properties for

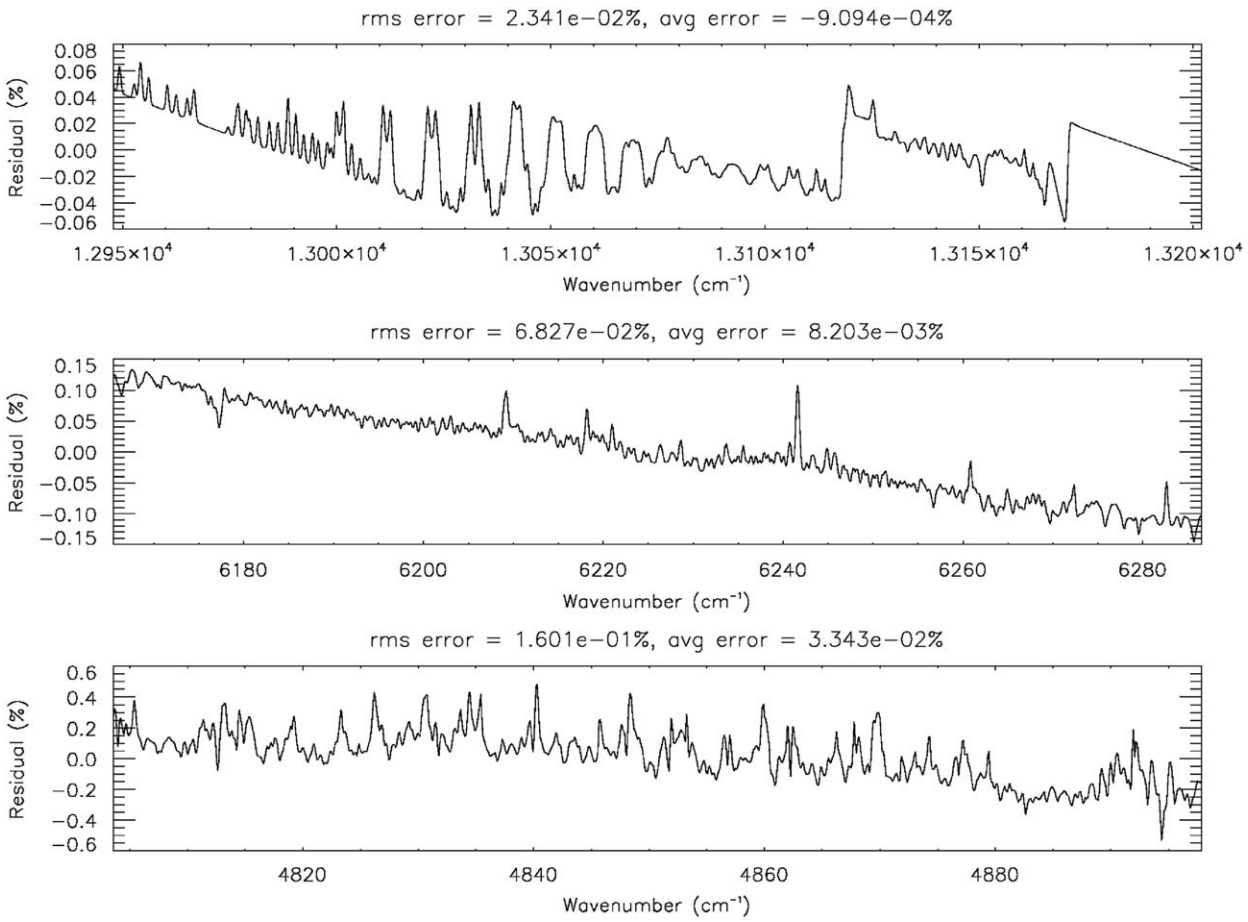

Fig. 3. Same as Fig. 1 but for *I*–*Q*.

Table 4
Root mean square (RMS) errors in the three spectral regions.

Scenario	% RMS error (O_2 *A* band)	% RMS error (1.61 μm CO_2 band)	% RMS error (2.06 μm CO_2 band)
28	0.003, 0.015, 0.003	0.001, 0.021, 0.001	0.005, 0.071, 0.005
174	0.009, 0.176, 0.011	0.017, 0.043, 0.019	0.022, 0.183, 0.019
256	0.022, 0.056, 0.023	0.066, 0.235, 0.068	0.158, 0.446, 0.160
2558	0.007, 0.030, 0.011	0.004, 0.094, 0.005	0.003, 0.052, 0.002

The three numbers in each cell correspond to the errors in Stokes parameters *I*, *Q* and *I*–*Q*, respectively.

Table 5
Timing details.

Scenario	RT time (s) (LBL)	RT time (s) (PCA)	Total time (s) (LBL)	Total time (s) (PCA)
28	4858.12	61.15	4875.28	83.45
174	5067.82	63.96	5096.67	96.08
256	5160.10	68.99	5193.31	105.34
2558	4875.67	61.99	4891.94	83.57

each bin. The slope goes away when a constant phase matrix is used. However, this effect can be ignored because the results are already of high accuracy. Second, the errors are higher for Stokes parameter *Q*. This is because for Stokes parameter *I*, we use the correlation between two-stream and *n*-stream intensities but do not

use a similar procedure for Q. The results for Q could be improved using a dedicated four-stream model and using the ratio of n-stream to four-stream values in the analysis. This would of course be at the expense of higher computational time. However, it is the degree of polarization that is usually significant and not the exact value of Q. In the continuum, this is usually low. In the line cores it can be high. However, this is a region which can be described by single scattering (which is computed exactly). Hence we expect the technique to work well as is. Third, the largest errors are in the 2.06 μm CO_2 band. This is a region with two significant absorbers (H_2O and CO_2). If we require greater accuracy, we would need to use additional bins for lines with large H_2O absorption, which would result in slightly higher computational time.

The monochromatic radiances have been convolved with a Gaussian with full width at half maximum (FWHM) 0.042481, 0.075825 and 0.097524 nm for the 0.76 μm O_2 A band, 1.61 μm CO_2 band and 2.06 μm CO_2 band, respectively, to simulate the finite spectral resolution of the satellite instrument.

Timing details are presented in Table 5. The RT computations are 70–80 times faster using PCA. If the total run time (that includes overheads due to input/output operations, phase matrix interpolation, binning, radiance mapping, etc.) is considered, the speed increase is about 50 fold. It is worth noting that the LBL computation time increases as the cube of the number of streams, while that for the PCA calculation is nearly independent of this quantity. Hence, the speed increase mentioned above is a lower bound. The computations were performed on a single node of a commodity Dell PowerEdge 1950 rack server with eight 2 GHz CPU cores, 8 GB of RAM and 12.5 TB of direct attached storage.

5. Conclusions

Line-by-line RT computations have a great deal of redundancy. This can be exploited by performing PCA on the optical properties and performing computationally expensive RT calculations on a small number of bins. We use this technique, along with a dedicated two-stream model and a highly efficient single scattering model to achieve speed increases of more than 50 fold relative to LBL computations while maintaining accuracies better than 0.1%. Since the choice of bins has to be done only once per spectral region, and does not depend on the details of the scenario, this technique can be implemented in operational retrieval algorithms.

Acknowledgments

The research described in this paper was performed for the Orbiting Carbon Observatory Project at the Jet Propulsion Laboratory, California Institute of Technology, under contracts with the National Aeronautics and Space Administration. This work was supported in part by NASA Grant NAG1-1806. The authors would like to thank the following people: Denis O'Brien, Igor Polonsky, Chris O'Dell and Adam Cardehen for sharing the ECMWF profiles; Hartmut Boesch for computing the optical property inputs for the RT calculations; Chris O'Dell for the convolution code; Jack Margolis, Mimi Gerstell and Nima Ghaderi for helpful comments on the manuscript.

References

[1] Natraj V, Jiang X, Shia R-L, Huang X, Margolis JS, Yung YL. Application of principal component analysis to high spectral resolution radiative transfer: a case study of the O_2 A band. JQSRT 2005;95(4):539–56. doi:10.1016/j.jqsrt.2004.12.024.

[2] Hasekamp OP, Landgraf J. Tropospheric ozone information from satellite-based polarization measurements. J Geophys Res 2002;107(D17):4326. doi:10.1029/2001JD001346.

[3] Hasekamp OP, Landgraf J, van Oss R. The need of polarization modeling for ozone profile retrieval from backscattered sunlight. J Geophys Res 2002;107(D23):4692. doi:10.1029/2002JD002387.

[4] Knibbe WJJ, de Haan JF, Hovenier JW, Stam DM, Koelemeijer PB, Stammes P. Deriving terrestrial cloud top pressure from photo-polarimetry of reflected light. JQSRT 2000;64(2):173–99. doi:10.1016/S0022-4073(98)00135-6.

[5] Koelemeijer RBA, Stammes P, Hovenier JW, de Haan JF. A fast method for retrieval of cloud parameters using oxygen A band measurements from the global ozone monitoring experiment. J Geophys Res 2001;106(D4):3475–90. doi:10.1029/2000JD900657.

[6] Liu X, Chance K, Sioris CE, Spurr RJD, Kurosu TP, Martin, RV, et al. Ozone profile and tropospheric ozone retrievals from the global ozone monitoring experiment: algorithm description and validation. J Geophys Res 2005;110(D20):D20307. doi:10.1029/2005JD006240.

[7] Rozanov VV, Kokhanovsky AA, Burrows JP. The determination of cloud altitudes using GOME reflectance spectra: multilayered cloud systems. IEEE Trans Geosci Remote Sens 2004;42(5):1009–17. doi:10.1109/TGRS.2004.825586.

[8] Schutgens NAJ, Stammes P. Parametrisation of Earth's polarisation spectrum in the ultra-violet. JQSRT 2002;75(2):239–55. doi:10.1016/S0022-4073(01)00248-5.

[9] Oshchepkov S, Bril A, Yokota T. PPDF-based method to account for atmospheric light scattering in observations of carbon dioxide from space. J Geophys Res 2008;113(D23):D23210. doi:10.1029/2008JD010061.

[10] Lacis AA, Chowdhary J, Mishchenko MI, Cairns B. Modeling errors in diffuse-sky radiation: vector vs. scalar treatment. Geophys Res Lett 1998;25(2):135–8.

[11] Mishchenko MI, Lacis AA, Travis LD. Errors induced by the neglect of polarization in radiance calculations for Rayleigh-scattering atmospheres. JQSRT 1994;51(3):491–510.

[12] Camp CD, Roulston MS, Yung YL. Temporal and spatial patterns of the interannual variability of total ozone in the tropics. J Geophys Res 2003;108(D20):4643–59. doi:10.1029/2001JD001504.

[13] Huang X, Farrara L, Leroy SS, Yung YL, Goody RM. Cloud variability as revealed in outgoing infrared spectra: comparing model to observation with spectral EOF analysis. Geophys Res Lett 2002;29(8):1270–3. doi:10.1029/2001GL014176.

[14] Peixoto JP, Oort AH. Physics of climate. New York: American Institute of Physics; 2002.

[15] Chandrasekhar S. Radiative transfer. New York: Dover; 1960.

[16] Crisp D, Atlas RM, Breon F-M, Brown LR, Burrows JP, Ciais, P, et al. The orbiting carbon observatory (OCO) mission. Adv Space Res 2004;34(4):700–9.

[17] Kuang Z, Margolis JS, Toon GC, Crisp D, Yung YL. Spaceborne measurements of atmospheric CO_2 by high-resolution NIR spectrometry of reflected sunlight: an introductory study. Geophys Res Lett 2002;29(15):1716–9. doi:10.1029/2001GL014298.

[18] Spurr RJD. Simultaneous derivation of intensities and weighting functions in a general pseudo-spherical discrete ordinate radiative transfer treatment. JQSRT 2002;75(2):129–75. doi:10.1016/S0022-4073(01)00245-X.

[19] Spurr RJD, Kurosu TP, Chance KV. A linearized discrete ordinate radiative transfer model for atmospheric remote-sensing retrieval. JQSRT 2001;68(6):689–735. doi:10.1016/S0022-4073(00)00055-8.

[20] Natraj V, Spurr RJD. A fast linearized pseudo-spherical two orders of scattering model to account for polarization in vertically inhomogeneous scattering-absorbing media. JQSRT 2007;107(2):263–93. doi:10.1016/j.jqsrt.2007.02.011.
[21] Natraj V, Spurr RJD, Bösch H, Jiang Y, Yung YL. Evaluation of errors from neglecting polarization in the analysis of O_2 *A* band measurements from space. JQSRT 2007;103(2):245–59. doi:10.1016/j.jqsrt.2006.02.073.
[22] Chevallier F. Sampled databases of 60-level atmospheric profiles from the ECMWF analyses. SAF Programme Research Report 4. EUMETSAT/ECMWF, Darmstadt, Germany, 2001.
[23] O'Brien DM, Polonsky I, O'Dell CW, Cardehen A. Orbiting Carbon Observatory (OCO) algorithm theoretical basis document: The OCO simulator. Technical Report. Cooperative Institute for Research in the Atmosphere, Fort Collins, CO, August 2009.